Journal of Structural Geology, Vol. 12, No. 7, pp. 869 to 882, 1990
Printed in Great Britain

0191-8141/90 $03.00 + 0.00
Pergamon Press plc

Formation of compound strike-slip fault zones, Mount Abbot quadrangle, California

S. J. MARTEL

Earth Sciences Division, Building 50E, Lawrence Berkeley Laboratory, University of California, Berkeley, CA 94720, U.S.A.

(*Received* 21 *March* 1989; *accepted in revised form* 4 *February* 1990)

Abstract—Numerous strike-slip fault zones in granitic rocks of the Mount Abbot quadrangle, California, developed from steeply-dipping, subparallel joints. These joints generally were less than 50 m long and were spaced several centimeters to several meters apart. Some joints subsequently slipped and became small faults. *Simple fault zones* formed as oblique dilatant fractures (splay fractures) linked non-coplanar faults side-to-side and end-to-end. These simple fault zones are as much as 1 km long and accommodated displacements as great as 10 m. *Compound fault zones* formed as splay fractures linked small faults and simple fault zones. They are as much as several kilometers long and accommodated displacements as great as 100 m. These zones are distinctly different from 'Riedel shear zones' and the mechanics of their formation are unlikely to be described well by Mohr–Coulomb mechanisms. Simple and compound fault zones are composed of non-coplanar segments that join at steps or bends; splay fracture length determines step widths. The longest splay fractures occur along the longest fault zones, allowing step widths to increase as the length and displacement across the zones increase. These findings are consistent with the structure of some active seismogenic faults, and they provide a mechanically consistent, field-based conceptual model for fault zones that grow in basement rocks from a pre-existing set of joints.

INTRODUCTION

FAULT zones commonly serve as long-standing zones of weakness in the Earth's crust, and the manner in which they form is highly relevant to important problems in earthquake mechanics and subsurface fluid flow. It is widely recognized that as fault zones develop in basement rocks they take advantage of pre-existing fractures (Hobbs *et al.* 1976, Price 1981, Davis 1984, Suppe 1985). However, because fault zones can be reactivated in different episodes of deformation under markedly different environmental conditions (Sibson, 1977, 1986, Sibson *et al.* 1981, McKee *et al.* 1984, Muehlberger 1986), the manner in which fault zones form from pre-existing fractures is commonly obscured. The scarcity of relatively simple, extensive exposures of fault zones in basement rocks is a major impediment to developing field-based models for how fault zones form (Logan *et al.* 1979). Indeed, the few well-defined conceptual models in the literature of structural geology that describe how fault zones grow are primarily based on laboratory model studies (Sylvester 1988). However, many of the laboratory simple shear experiments have been directed towards how fault zones develop in the sedimentary sequences overlying a pre-existing basement fault (e.g. Naylor *et al.* 1986); how the basement faults themselves develop remains an open question. Field observations are essential to test to what extent laboratory simple shear models can be applied to large natural fault zones in basement rocks.

This paper presents a model for how *compound strike-slip fault zones* formed from pre-existing fractures within plutons of the Mount Abbot quadrangle in the Sierra Nevada of California (Fig. 1). This area provides a rare opportunity to track the development of fault zones from their inception for three main reasons: (1) faulting developed to different stages in different parts of the quadrangle; (2) the effects of subsequent deformation are minimal and (3) exhumed strike-slip faults and fault zones are well displayed. The smallest faults in the area are a few meters long, a few millimeters thick and accommodated less than 1 cm of strike-slip displacement, whereas the largest compound fault zones are several kilometers long, several meters thick and accommodated approximately 100 m of strike-slip displacement. Two exposures of compound fault zones were mapped in detail, one at the Waterfall site and another at the Seven Gables site (Fig. 1); these fault zones are decidedly different from the structures that have been formed in many laboratory simple shear experiments. The paper concludes with a discussion of how the Bear Creek fault zones formed, contrasts that model with the results of laboratory simple shear experiments, and addresses some of the seismic implications of the model.

Before proceeding further, the use of a few terms in the paper is clarified. Fractures are classified as either joints or faults in the manner suggested by Engelder (1987). The term 'joint' is used where there is clear evidence for a lack of appreciable shear displacement across a fracture, and the term 'fault' is used where there is clear evidence of appreciable shear displacement. The more general term 'fracture' is used where there is not clear evidence on whether or not there was shear displacement. Adjacent segments of a fault zone may join at steps or bends (Fig. 2c). Parallel but not coplanar segments join at a 'step', and adjacent segments of different orientation join at 'bends'. Steps and bends are referred to collectively as systematic geometric discontinuities.

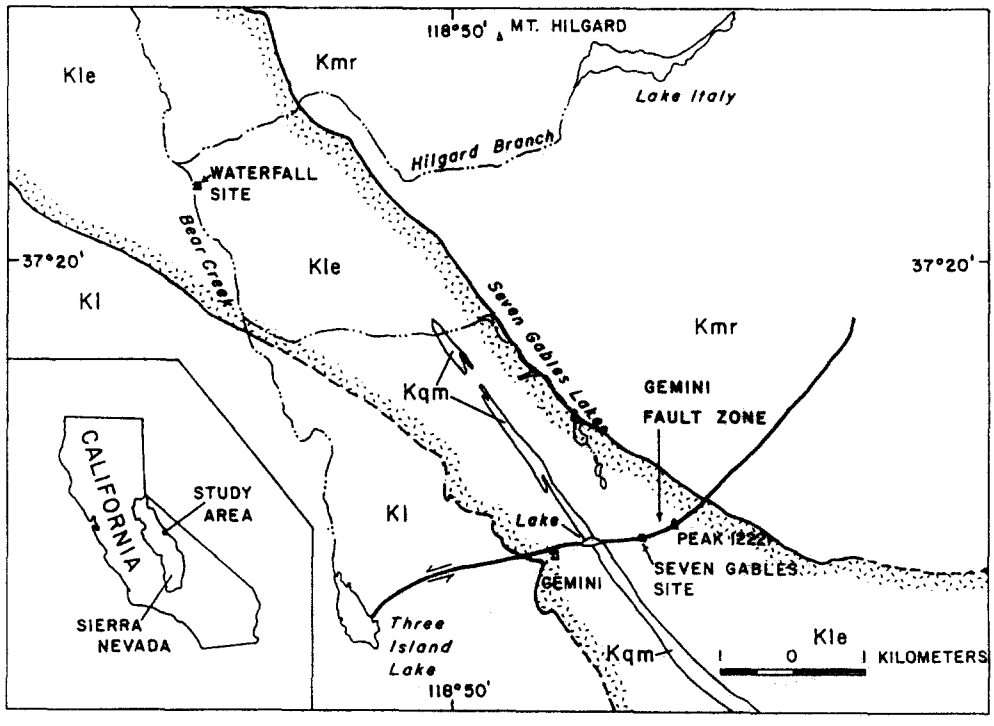

Fig. 1. Geologic map of the area of study in the Mount Abbot quadrangle. Geology generalized from Lockwood & Lydon (1975). Kl = Cretaceous Lamarck grandodiorite; Kle = Cretaceous granodiorite of Lake Edison; Kmr = Cretaceous quartz monzonite of Mono Recesses. Geologic contacts are dashed where locations are approximate. The nearly vertical quartz monzonite body (Kqm) is displaced approximately 70 m across the Gemini fault zone. Triangles show locations of landmark peaks.

GEOLOGIC SETTING

The study area is in the Bear Creek region of the Mount Abbot quadrangle and includes three adjacent NW-trending plutons (Fig. 1) mapped and described by Lockwood & Lydon (1975). Field relations show that the westernmost pluton (the Lamarck granodiorite) is the oldest, that the central pluton (the granodiorite of Lake Edison) is of intermediate age, and that the easternmost pluton (the quartz monzonite of Mono Recesses) is youngest. Based on K–Ar dating of biotites, these plutons have ages of 79–85, 77–82 and 79–82 Ma, respectively (Stern *et al.* 1981). These ages provide maximum ages for the fault zones. All three plutons contain a weak, steeply-dipping foliation that strikes NW. Mineralized joints, faults and fault zones that strike ENE are abundant within the older two plutons. Mineralized joints that strike ENE are also abundant within the Mono Recesses pluton, but faults and fault zones that strike ENE appear scarce. Considering the likely origin and evolution of the faults and fault zones (discussed below), their distribution suggests that the faulting in the older two plutons may have occurred before or during emplacement of the Mono Recesses pluton. The faults would then have formed at the depth of emplacement. Work by Noyes *et al.* (1983) indicates that the nearby and nearly contemporaneous Eagle Peak and Red Lake plutons were emplaced at a depth of approximately 4 km.

The first three stages of faulting in the Bear Creek area (Figs. 2a–c) have been discussed recently by Martel *et al.* (1988). The faults and fault zones developed from steeply-dipping subparallel joints (Segall & Pollard 1983a,b). Hydrothermal minerals fill the joints, epidote and chlorite being particularly common. Those joints not involved in subsequent deformation contain undeformed minerals. Joint spacing and joint length range from a few decimeters to a few tens of meters. The joints typically are 0.1–10 mm thick.

During the second stage of deformation some joints slipped and became small left-lateral faults (Fig. 2b), offsetting xenoliths and steeply-dipping aplite dikes by as much as 2 m (Segall & Pollard 1983b, Martel *et al.* 1988). Not all joints in a given outcrop slipped, so unslipped joints parallel adjacent small faults. Slickenlines on the fault surfaces typically plunge less than 20°, indicating that at least the most recent displacements on the faults were dominantly strike-slip (Segall & Pollard 1983b). As a result of slip, the material in these faults acquired mylonitic fabrics, and NNE-striking fractures (*splay fractures*) opened near fault ends. The splay fractures are filled primarily by epidote, chlorite and quartz. Although some splay fractures are several meters long, they rarely extend more than a few meters away from the faults. The splay fractures are inferred to strike in the direction of the maximum horizontal compressive stress (Segall & Pollard 1983b). Some originally unconnected left-stepping echelon faults were linked by splay fractures, whereas some right-stepping echelon faults were linked by ductile deformation of the intervening rock. Linked echelon faults are as much as several hundred meters in length and accommodated left-lateral displacements as great as several meters.

Larger left-lateral displacements were accommodated

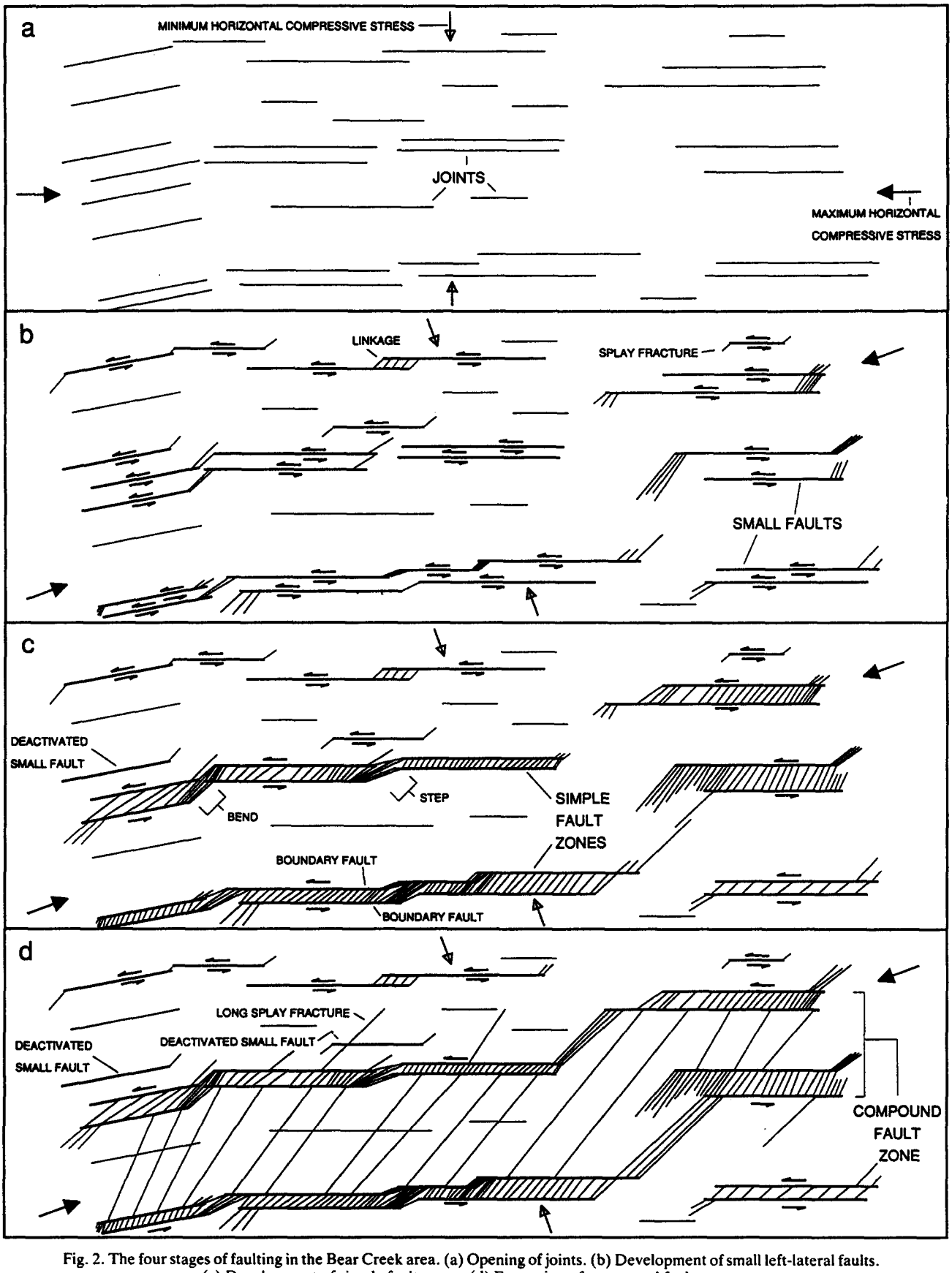

Fig. 2. The four stages of faulting in the Bear Creek area. (a) Opening of joints. (b) Development of small left-lateral faults. (c) Development of simple fault zones. (d) Formation of compound fault zones.

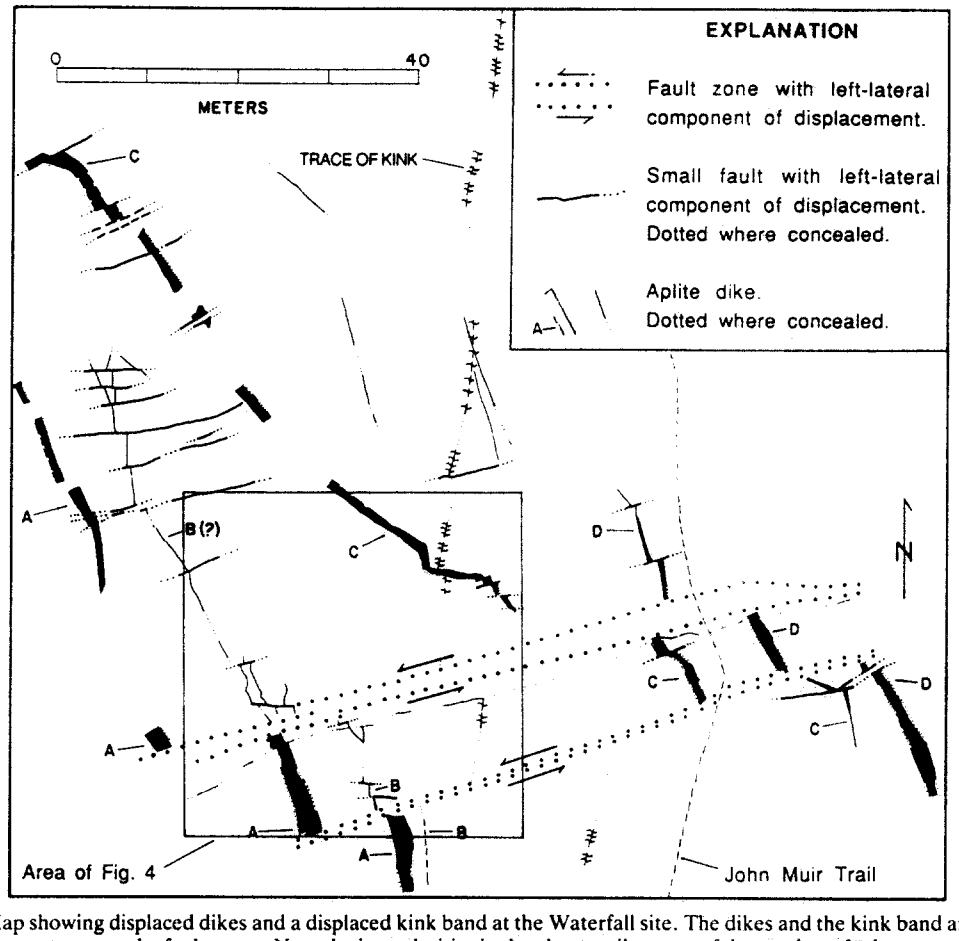

Fig. 3. Map showing displaced dikes and a displaced kink band at the Waterfall site. The dikes and the kink band are offset similar amounts across the fault zones. Note the irregularities in the along-strike trace of the northern fault zone near dikes A and D.

in the third stage of deformation (Fig. 2c) as abundant fractures linked faults side-to-side to form *simple fault zones* (Martel *et al.* 1988). The fractures within these zones contain epidote, chlorite and quartz, with smaller amounts of muscovite and calcite. The most prominent fractures strike obliquely to the sharply defined faults (the boundary faults) at the edges of the zones. The rock inside a zone is highly fractured, in sharp contrast to the relatively unfractured rock immediately outside. Simple fault zones typically are 0.5–3 m thick and up to 1 km long. Their traces consist of straight, non-colinear segments a few tens of meters long that join at steps or bends. This indicates that non-coplanar small faults linked end-to-end to form the boundary faults of simple fault zones. The maximum strike-slip displacement observed across a simple fault zone is about 10 m. The displacement is concentrated on the boundary faults.

STRUCTURE OF COMPOUND FAULT ZONES

Waterfall site

The Waterfall site lies along the north edge of a network of faults and fault zones that left-laterally separates steeply-dipping aplite dikes and compositional layering in the granodiorite by several tens of meters. This network is a few tens of meters wide, is well exposed over a horizontal distance of 500 m, and crops out over a vertical interval of at least 300 m.

Two prominent sets of steeply-dipping mineralized fractures occur at the site (Figs. 3 and 4). The first set consists of joints, small faults and two fault zones. These strike 060–075°. The second set consists of mineral-filled fractures that strike NNE. Fractures in the second set are present across the site, but are most common near the fault zones.

A kink band with axial planes that strike 010° deflects some of the joints and faults in a right-lateral sense (Figs. 3 and 4). The spacing between the kinked joints and faults generally is less than 20 cm, whereas away from the kink band the spacing generally ranges from about 20 cm to 3 m. Similar kink bands occur elsewhere in the Bear Creek region (Segall & Pollard 1983a, Davies & Pollard 1986, Martel *et al.* 1988). The right-lateral deformation along the kink bands is interpreted as conjugate to the left-lateral displacement across the faults and fault zones.

The two fault zones at the site (Figs. 3 and 4) appear to offset the kink band, giving a left-lateral strike separation of several meters. Prominent aplite dikes also have left-lateral strike separations of about 10 m across each fault zone. The fault zones are 2–3 m thick and are

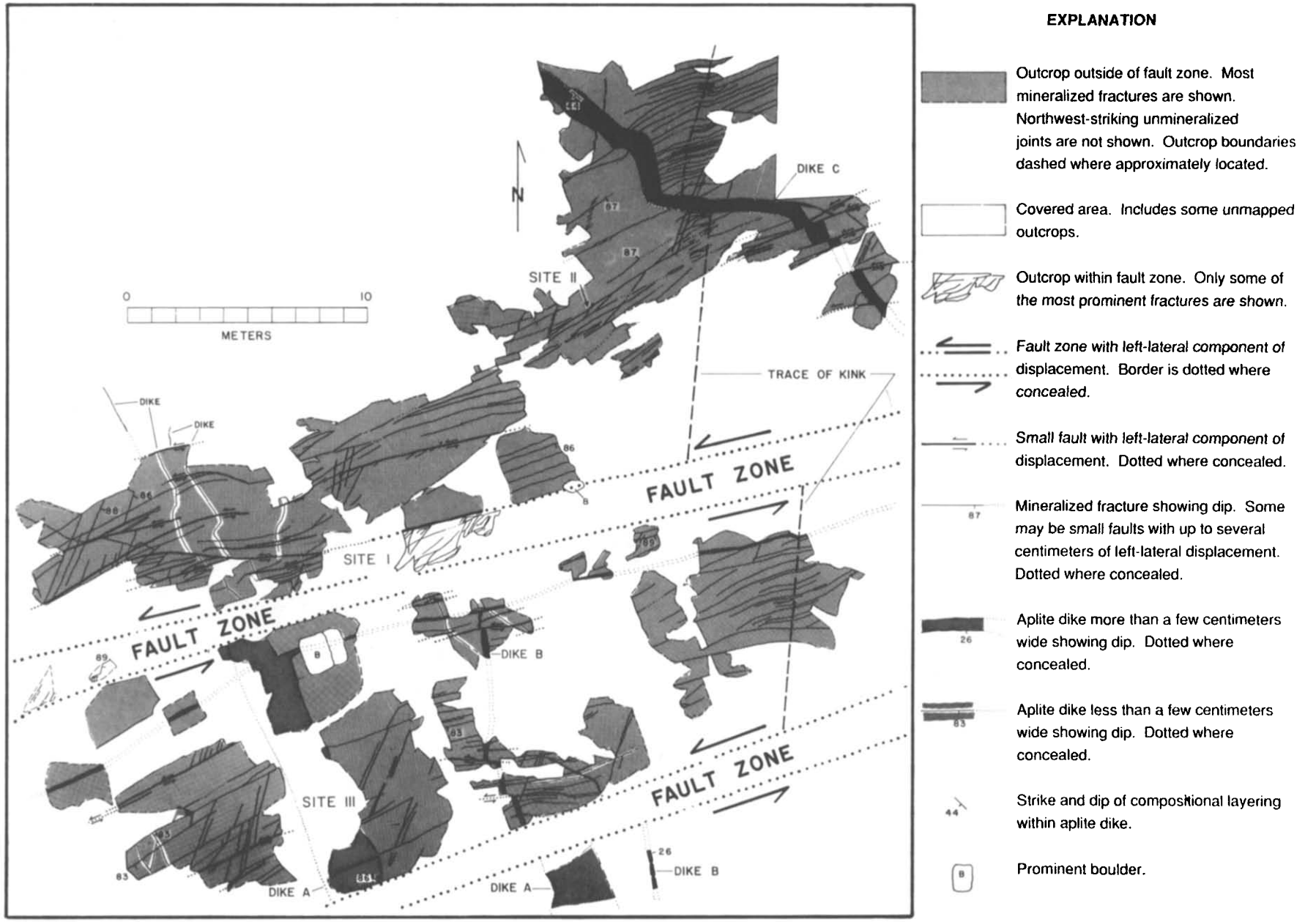

Fig. 4. Map showing joints, faults and fault zones at the Waterfall site. Sites I, II and III are referred to in the text.

spaced 7–14 m apart. The rock exposed inside each fault zone is highly fractured, whereas the rock immediately adjacent to the zones is little-fractured (Fig. 5). The fractures contain epidote, chlorite, quartz, calcite and white mica. The topographic expression of the fault zones as shallow troughs indicates that internal fractures are abundant along the length of the fault zones.

The boundaries of the northern fault zone do not form straight traces across the Waterfall site. Instead, the fault zone is segmented along strike, making a left-step at site I of Fig. 4 and a bend of ~10° near dike D of Fig. 3. The segment defined is ~50 m long. The northern boundary fault of this zone has a maximum exposed thickness of 1 cm. Like all other boundary faults sampled in the Bear Creek region, it has a cataclastic texture, with angular fragments of quartz and feldspar set in a dark green–brown, fine-grained, isotropic matrix. The cataclastic texture contrasts sharply with the mylonitic fabrics of small faults (Segall & Pollard 1983b).

Two subsets of mineral-filled dilatant fractures strike NNE at the Waterfall site. The first subset comprises fractures that are no more than several decimeters long and contain epidote, quartz and chlorite. They typically branch from small faults (site II, Fig 4) and are referred to as *splay fractures*. They are interpreted as forming in response to slip on the small faults (Segall & Pollard 1983b). Fractures of the second subset typically are 1–4 m long and are bordered by halos of hydrothermally altered rock (site III, Fig. 4). These long fractures are common only between or alongside the two fault zones and are interpreted as being splay fractures that formed in response to slip on the fault zones. Some of the long splay fractures are continuous structures, whereas others are bands of short echelon cracks. Some of these fractures cross small faults; most are not offset by the faults, although some appear to be offset slightly (less than 2 mm). These relationships support the interpretation that the long fractures formed during the episode of faulting, but indicate that the long splay fractures formed after all or nearly all of the slip on the small faults had occurred. Because the long NNE-striking fractures do not visibly offset the small faults they are interpreted as dilatant fractures. Long NNE-striking fractures have been observed along other fault zones in the Bear Creek area, but only along those that accommodated displacements of at least 10 m.

The Gemini fault zone and the Seven Gables site

The Gemini fault zone (Fig. 1) is the largest fault zone mapped by Lockwood & Lydon (1975) within the Mount Abbot quadrangle. The topographic trough marking the fault zone is generally about 10 m wide and extends over an elevation range of approximately 700 m. However, neither the top nor the bottom of the fault zone is exposed, so the fault zone could have a vertical extent much greater than 700 m. The zone is about 10 km long and has a sigmoidal shape in plan view. The 4 km long central limb strikes approximately 075° and dips steeply to the north. The east and west limbs strike NE. Near the east end of the central limb the fault zone offsets a steeply-dipping quartz–monzonite body ~70 m in a left-lateral sense (Fig. 1). Some steeply-dipping dikes are offset left-laterally by about 100 m near the west end of the central limb (Lockwood & Lydon 1975).

Examinations of several outcrops along the Gemini fault zone indicate that it contains a series of faults that are subparallel to the zone as a whole. These faults divide the zone into a series of fractured bands. The intensity of fracturing and the degree of chemical alteration varies from one band to another. Fractures striking oblique to the fault zone typically are scarce in the rock immediately adjacent to the zone.

The largest identified exposure of the Gemini fault zone occurs along its central limb (Fig. 1). The northern part of the fault zone was mapped in detail at that outcrop (Fig. 6); the southern part of the zone is covered by talus. The fault zone does not have a straight trace near this outcrop. The fault zone strikes approximately 080° over a 40–50 m interval at the outcrop and dips approximately 70° to the north. Immediately east of the exposure, the fault zone bends to a strike of ~065°. Several meters west of the outcrop, the fault zone steps several meters to the south. The fault zone thus consists of segments that are not coplanar.

The rock north of the fault zone contains two major sets of mineralized fractures (Fig. 6). The first set consists of fractures that parallel the fault zone and contain epidote and chlorite. The spacing between these fractures typically is half a meter to a few meters, similar to the spacing between ENE-striking fractures at the Waterfall site. Some of the fractures appear to be joints, but others are faults with slickenlines. The second set comprises fractures that strike 010–050° and dip steeply to the east. Some are several meters long. Fractures of the second set appear to be dilatant cracks, for they cross fractures of the first set but do not offset them laterally. This set has three subsets: continuous fractures, bands of short echelon cracks and ribs of hydrothermally altered granitic rock. These fractures are concentrated near the fault zone and are interpreted to have formed in association with slip on the zone.

The Gemini fault zone itself is divided into fracture-bounded bands of markedly different fracture intensity (Figs. 6 and 7). The fractures bounding the bands almost certainly are all faults, but a lack of markers prevented the amount of displacement across them from being documented. Four bands are exposed, but additional bands might exist beneath the talus that covers the southern part of the fault zone. The first and northernmost band is about 80 cm thick, has an exposed length of 3 m, and contains highly fractured rock. Prominent fractures within the band strike ~35° counterclockwise from the band boundaries and cut an aplite dike but do not offset it laterally. This band appears to be a relict simple fault zone. The second band is about 1 m thick and is exposed over an interval about 10 m long. The intensity of fracturing within this band (Fig. 7b) is markedly less than that of the first band and is similar to

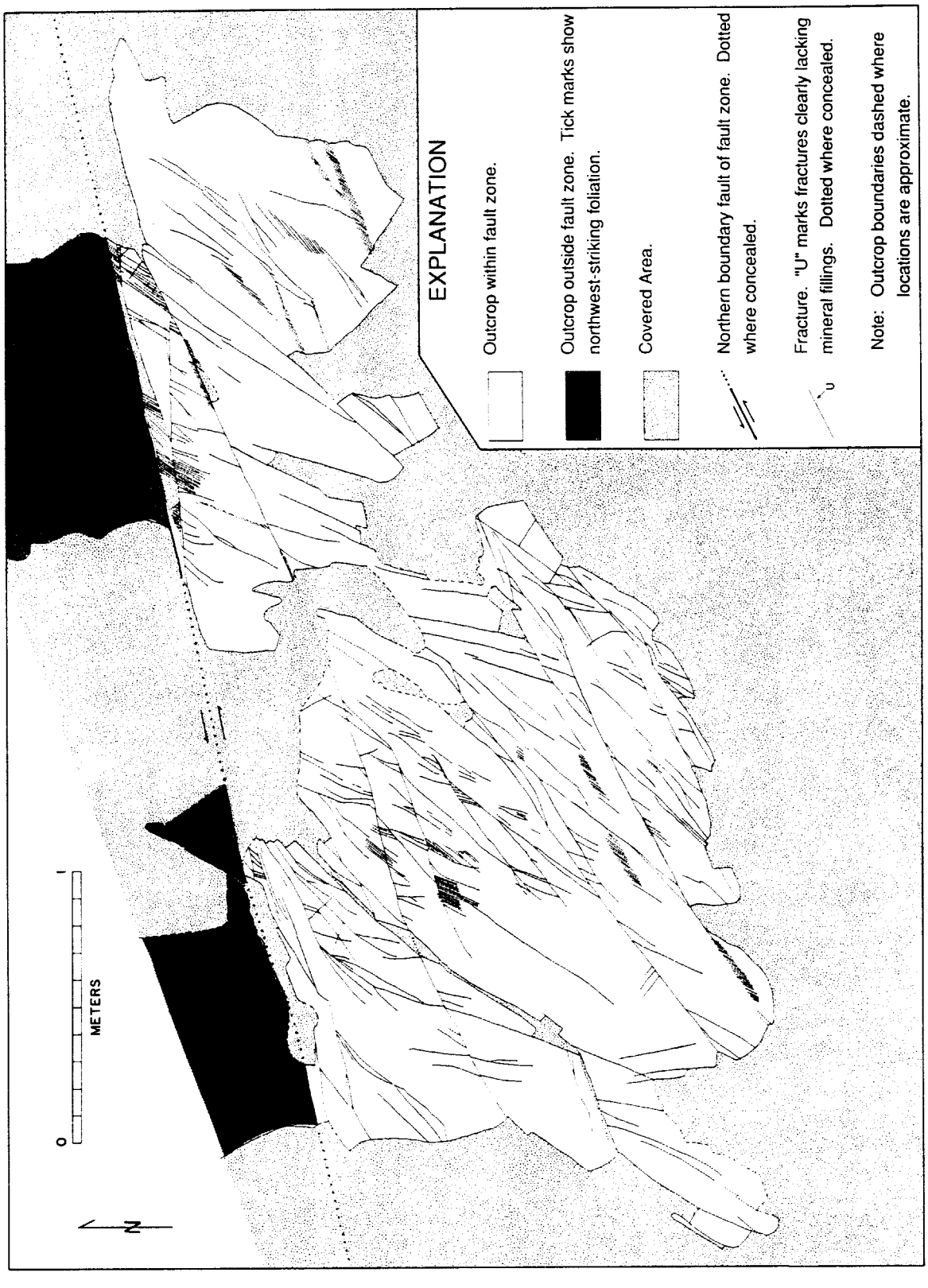

Fig. 5. Map of fractures within a small outcrop in the northern fault zone at the Waterfall site. This outcrop is located just east of the left-step in the fault zone.

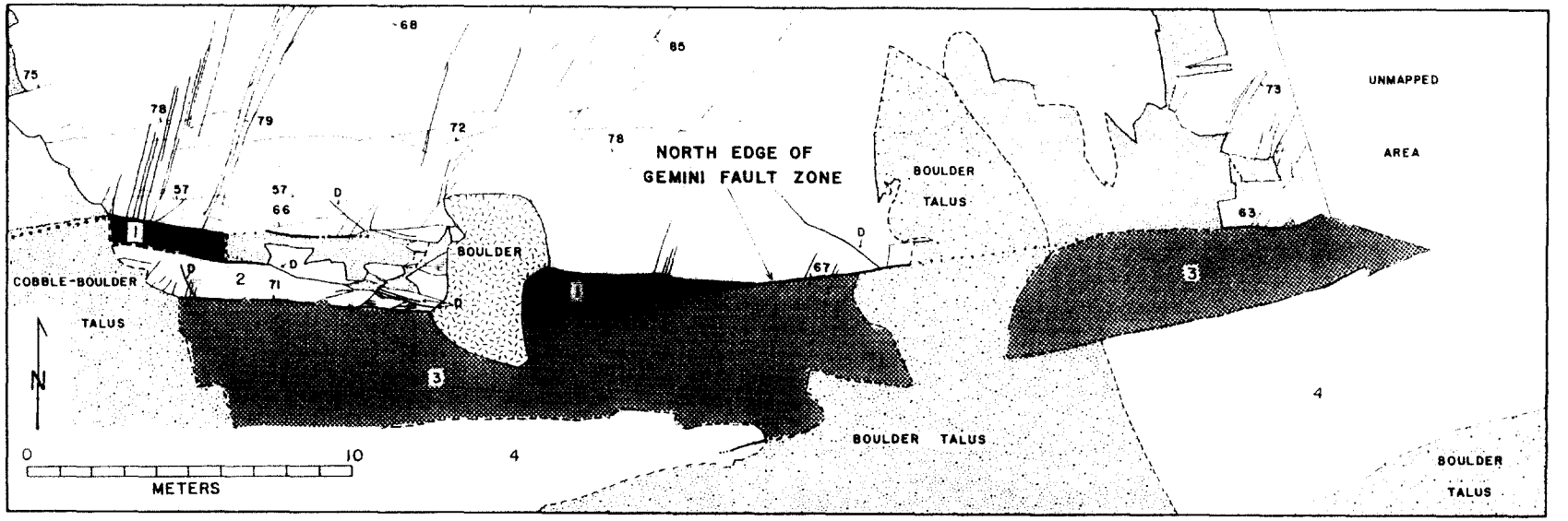

EXPLANATION

Outcrop showing mineralized fractures. Northwest-striking unmineralized joints are not shown.

Band of angular blocks mostly 5-100 cm in diameter.

Band of angular blocks mostly 5-100 cm in diameter with chlorite-coated surfaces.

Band of angular fragments mostly less than 20 cm in diameter with chlorite-coated surfaces.

Talus.

Area covered by granitic sand and angular pebble-sized fragments.

Contact, dashed where location is approximate.

Fault, showing dip. Dashed where location is approximate, dotted where concealed.

Mineralized fracture showing dip. The fractures are planar; the "staircase topography" of the outcrop causes many of the fracture traces to be nonlinear. Dotted where concealed.

Band of echelon fractures showing dip of band.

Raised rib of hydrothermally altered granodiorite showing dip.

Aplite dike. Dotted where concealed.

Prominent boulder.

Fig. 6. Map of fractures along the northern margin of the Gemini fault zone at the Seven Gables site.

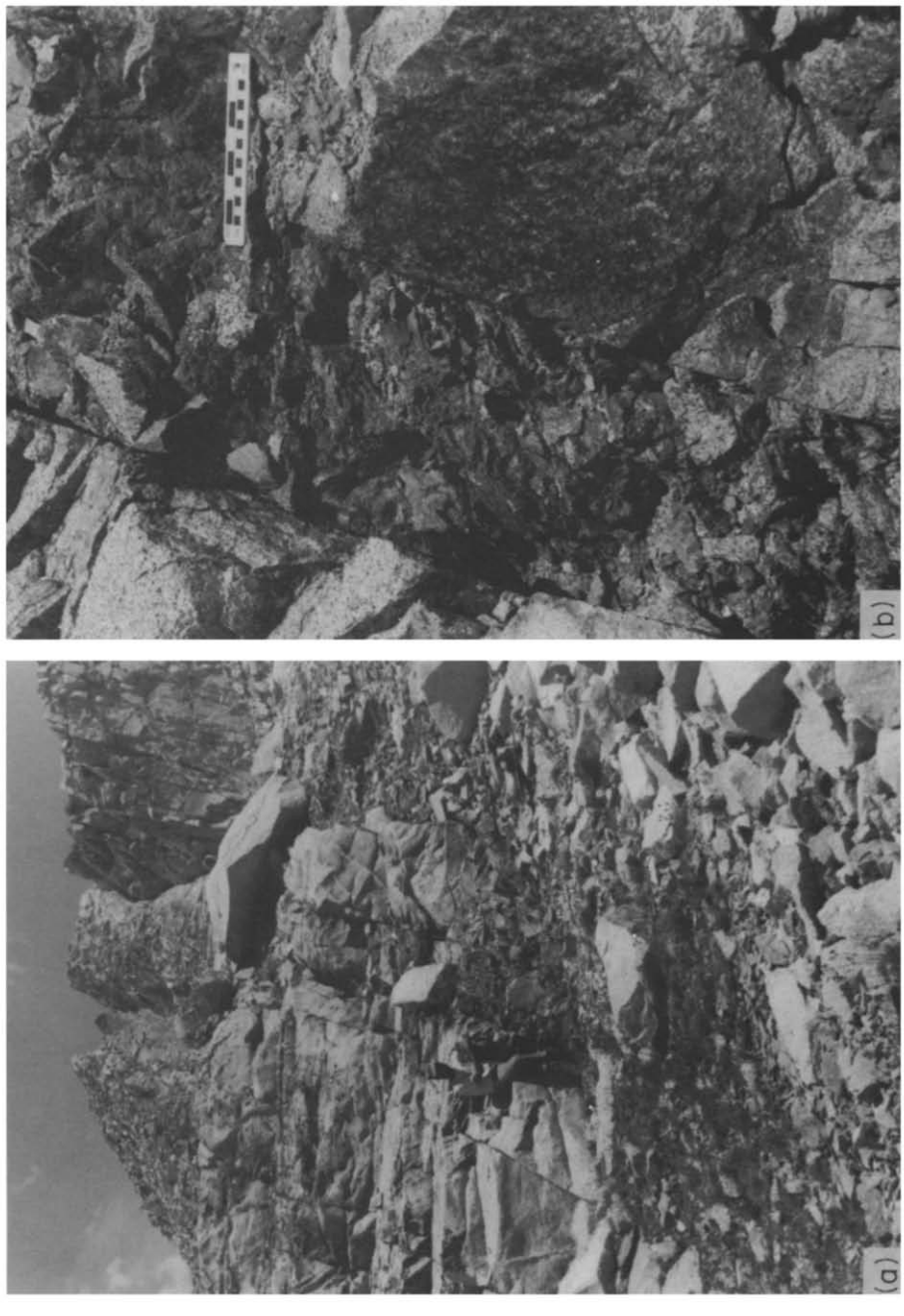

Fig. 7. Views to the east of the Seven Gables outcrop along the Gemini fault zone. (a) Distant view. Trace of Gemini fault zone passes through the largest notch in skyline. The 15 cm scale of (b) is on the light-colored block to the right of the geologist's boots. (b) Close-up view of west end of outcrop showing bands 1 and 2 of Fig. 6.

that in the rock outside the fault zone. The third band is 1–4 m thick and consists of chlorite-coated fragments 5–25 cm long. Where exposed at the east end of the outcrop, the contact between the third and fourth bands is a fault with a cataclastic texture. This fault strikes parallel to the zone. The fourth band is at least 5 m thick and consists of cobble- to boulder-size blocks that generally lack chloritic coatings.

A MODEL FOR THE GROWTH OF COMPOUND FAULT ZONES

The fault zones that extend through the Waterfall and Seven Gables sites are larger and have accommodated more displacement than simple fault zones. For example, most simple fault zones appear to be several hundred meters long, less than a few meters thick and have accommodated less than 10 m of lateral displacement. In contrast, the Gemini fault zone is several kilometers long, approximately 10 m thick and has accommodated ~100 m of lateral displacement; its dimensions are approximately an order of magnitude greater than a simple fault zone. The Gemini fault zone and the network of faults at the Waterfall site are also structurally more complex than simple fault zones. Along a simple fault zone (Fig. 2c), two boundary faults are linked side-to-side. Internal faults that parallel the boundaries of a simple fault zone are rare. In contrast, the Gemini fault zone incorporates many internal faults that parallel its boundaries, and for that reason is referred to here as a *compound fault zone* (Fig. 2d). The fault network at the Waterfall site is interpreted to be of an intermediate nature, for small faults and simple fault zones are distinct, but long oblique fractures connect some of the simple fault zones side-to-side. The fault network at the Waterfall site can therefore be regarded as a compound fault zone deactivated at an earlier stage of development than the Gemini zone.

Despite their differences in size, the across-strike structure of both simple and compound fault zones reflects a distribution of joints similar to that in local unfaulted outcrops. Both kinds of zones are paralleled by steeply-dipping small faults and joints. ENE-striking fractures inside and outside the Gemini fault zone (Fig. 6), as well as those in the vicinity of the Waterfall site (Figs. 3 and 4), are generally spaced several decimeters to a few meters apart. This is comparable to the spacing of joints and the thicknesses of simple fault zones throughout the Bear Creek region (Segall & Pollard 1983a,b, Martel *et al.* 1988) and indicates that compound fault zones developed from arrays of joints. The compound fault zones apparently did not develop from joints with either an usually close or unusually wide spacing, *nor did the growth of the zones involve the generation of new fractures parallel to the zone.* The across-strike structure of compound fault zones thus indicates that many already existing fractures were *incorporated* into the fault zones as they grew in thickness.

The segmented along-strike structure of compound fault zones also reflects the distribution of joints in local unfaulted outcrops. The segment of the Gemini fault zone at the Seven Gables exposure and the segment in the northern fault zone at the Waterfall site are both 40–50 m long (Fig. 3). The principal fractures in the network of faults east of the Waterfall site usually are no more than several tens of meters long. The longer joints in local outcrops also have maximum lengths of several tens of meters (Segall & Pollard 1983a). It seems that the simple and compound fault zones preferentially developed from joints several tens of meters long. Perhaps these long joints were able to slip more readily than shorter ones. The thickness of the fillings in the joints appears to scale approximately with joint length, so opposing faces of a joint are less likely to interlock the longer a joint is. Still, the formation of fault zones several kilometers long apparently did not require the presence of joints several kilometers long.

The evolution of faulting in the Bear Creek area (Fig. 2) largely reflects the linkage of non-coplanar structures by fractures. As a result, faults and fault zones have systematic discontinuities along strike. The scale of these discontinuities increased as the faulting progressed. Small faults evolved from joints. Detailed examinations (Segall & Pollard 1983a) show that the joints themselves are not perfectly planar structures. Instead, they consist of numerous parallel echelon strands spaced less than a few centimeters apart. When a joint subsequently slipped and became a small fault, these strands were linked. The discontinuities along the strike of a small fault thus have amplitudes of less than a few centimeters. Simple fault zones formed as small faults linked side-to-side and end-to-end. As a result, these zones are segmented along strike. Adjacent segments join at steps as wide as a few meters or at bends of as much as 20° (Martel *et al.* 1988). Discontinuities along the strike of simple fault zones thus have amplitudes of a few meters at spacings of several tens of meters. The formation of compound fault zones involves the linkage of simple fault zones by fracturing. Because splay fractures along compound fault zones can be several meters long, steps along the strike of compound fault zones can have widths of several meters.

The distribution of fractures along the faults and fault zones of the Bear Creek area thus can reveal the extent to which geometric discontinuities affected slip as the faulting progressed. Experimental work (Erdogan & Sih 1963, Brace & Bombolakis 1963, Horii & Nemat-Nasser 1985) and theoretical studies (Erdogan & Sih 1963, Pollard & Segall 1987) indicate that splay fractures would form along faults where displacement gradients (i.e. strains) and the associated stress concentrations become sufficiently large. Splay fractures along small faults are concentrated only near the fault ends, indicating that the discontinuities along the small faults did not act to produce large displacement gradients. Along simple fault zones, fractures are abundant in the adjacent rock only near the ends of segments (Martel *el al.* 1988). The geometric discontinuities at segment ends were of sufficient size to cause steep displacement gradi-

ents as the boundary faults slipped. The geometric discontinuities along compound fault zones can be considerably larger than those along simple fault zones, so one would expect that steep displacement gradients would also develop at the large discontinuities along the compound fault zones as they slipped.

These discontinuities along the simple and compound fault zones did not present permanent barriers to slip. The displacements across adjacent segments of some simple fault zones appear to be nearly equal (Martel *et al.* 1988). The strike separations of steeply-dipping features near the east and west ends of the 5 km long central limb of the Gemini fault zone are also similar. The similar strike separations at different places along the fault zones implies that the discontinuities along the zones become broken during the growth process and allow displacement to be transferred along the zones.

DISCUSSION

Perhaps the most often cited classification scheme for fault zone fractures is that of 'Riedel shears' (e.g. Logan *et al.* 1979, Swanson 1988, Sylvester 1988). This classification scheme (Fig. 8) is an outgrowth of the 'clay cake' experiments made famous by Cloos (1928) and Riedel (1929) and subsequently conducted by a host of others (Sylvester 1988). Most of these experiments have been conducted in soft fine-grained materials under low confining pressure, but experiments with simulated fault gouge under high confining pressures (Logan *et al.* 1979) and with limestone (Bartlett *et al.* 1981) have produced similar fracture patterns. The fracture patterns from the simple shear experiments usually have been interpreted in light of Mohr–Coulomb shear failure criteria (Tchalenko 1968, 1970, Logan *et al.* 1979, Sylvester 1988). Fracture patterns similar to those produced in the laboratory experiments have been observed in weakly consolidated surficial deposits along natural faults as long as several hundred kilometers (Tchalenko & Ambraseys 1970, Sylvester 1988) and in some fault zones in metamorphic basement rocks (Swanson 1988). Because of the similarity of the laboratory and natural fracture patterns it is appealing to apply Riedel shear terminology and Mohr–Coulomb criteria to explain the field observations. However, as Logan *et al.* (1979) pointed out in describing their experiments "... it should be emphasized that these experiments were not designed as scale models of larger fault zones. They were envisioned as attempts to look at the processes in simulated fault zones of a few centimeters displacement. It was hoped that if the processes operating in the laboratory specimens could be understood that some aspects might prove to be scale independent and thus could be applied to larger natural faults, but there is no *a priori* reason why this should be so . . .".

The compound fault zones of Bear Creek do not fit well into the Riedel shear classification. First, the sequences of fracturing are completely different (Figs. 2 and 9). The zone-parallel faults of the simple and compound zones predate the obliquely-striking fractures within and along the zones. In contrast, the zone-parallel *Y*-shears in the simple shear experiments are typically among the last fractures to form (Wilcox *et al.* 1973, Bartlett *et al.* 1981, Naylor *et al.* 1986). Second, the most prominent fractures in and along the Bear Creek fault zones appear to have originated as dilatant fractures and not shear fractures. The evidence that the zone-parallel faults of the simple and compound fault zones originated from joints is compelling. The long NNE-striking splay fractures associated with the compound fault zones also originated as dilatant fractures. Most of the long NNE-striking fractures strike 60°–70° counterclockwise relative to the faults; this is the orientation at which antithetic (*R'*) Riedel shears would be expected based on a simple shear model (Sylvester 1988). The fractures within the first fault zone band at the Seven Gables outcrop cross but do not offset an aplite dike and they strike at 35° to the faults bounding the band. Only the T fractures of the simple shear

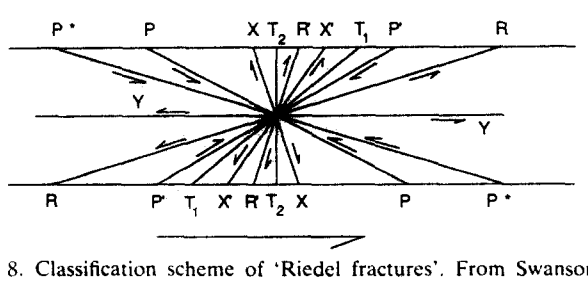

Fig. 8. Classification scheme of 'Riedel fractures'. From Swanson (1988).

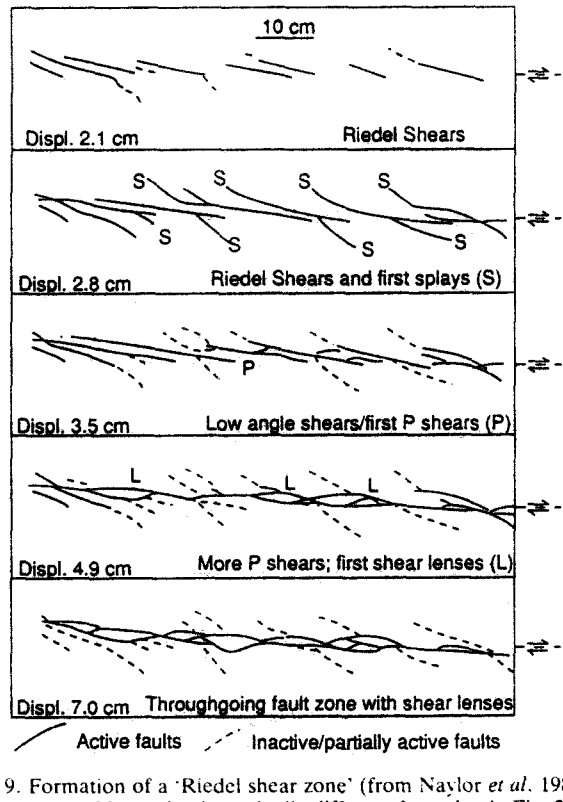

Fig. 9. Formation of a 'Riedel shear zone' (from Naylor *et al.* 1986). Sequence of fracturing is markedly different from that in Fig. 2.

models do not show shear displacements, but they strike at 45° or 90° to the zone, not 35°. Thus the relative age, the mode of formation and the orientation of the first-order features of the compound fault zones do not fit within a Riedel simple shear model. Finally, and perhaps most importantly, the spatial organization of the fractures in the fault zones (Fig. 2) is not addressed in the Riedel classification scheme (Fig. 8).

The linkage model of Fig. 2 is consistent with the field observations of the compound fault zones and readily allows the zones to be considered in the context of fracture mechanics (e.g. Martel & Pollard 1989). In this model the zone-parallel faults originate as joints. Left-lateral slip along these faults is predicted to generate dilatant fractures that strike in the general direction of the maximum horizontal compressive stress, that is at acute counterclockwise angle to the faults (Martel & Pollard 1989). Dilatant splay fractures with a range of orientations would not be inconsistent with such a model given the heterogeneity of the stress field that could exist along a fault zone with a non-linear trace (e.g. Segall & Pollard 1980, Billham & King 1989). Fracture mechanics theory predicts that fractures splaying from left-lateral faults should not strike at acute clockwise angles to the faults, and this is consistent with the field observations. Dilatant fractures produced as a result of slip on the zone-parallel faults could subsequently accommodate slip themselves, which could in turn lead to the generation of another order of dilatant fractures (e.g. Martel *et al.* 1988).

Many natural fault zones in addition to those of the Bear Creek area appear to become thicker as they accommodate greater displacements (Aydin & Johnson 1978, Robertson 1983, Wallace & Morris 1986, Scholz 1987). Microstructural observations suggest that the process of thickening at the grain-scale level commonly occurs by a diffuse front of brittle deformation migrating laterally into the host rock. Friction experiments with orthoquartzite (Hundley-Goff & Moody, 1980), sandstone (Engelder 1974) and crystalline rock (Jackson & Dunn 1974) show that artificial faults can increase in thickness as grains in the host rock adjacent to the fault become fractured and then incorporated into the fault. A similar process apparently operated over distances of a few grain diameters along the boundary faults in the Mount Abbot quadrangle (Martel *et al.* 1988). Such a process may also operate at a much larger scale. Within both the White Rock thrust fault in Wyoming (Mitra 1984) and the Punchbowl Fault of the San Andreas system (Chester & Logan 1986), deformation is greatest in the middles and decreases towards the margins. The intensity of deformation in ductile shear zones also commonly decreases away from the center of the zone (Ramsay 1980, Segall & Simpson 1986). These observations suggest that many natural fault zones and shear zones have thickened as a diffuse front of brittle or ductile deformation migrated from a central weak zone into the host rock.

The compound fault zones do not seem to have thickened by a 'diffusive' process. The compound zones thickened as fractures linked small faults and simple fault zones, with thickening occurring in *increments* determined by the initial joint spacing and the distance that splay fractures could propagate. This process allows deformation to be most intense at the edges of a fault zone rather than in its center, while still enabling the zone to maintain sharp boundary faults. In contrast to the processes of frictional wear, as the compound fault zones grew and the displacement increased, the width of steps along strike became larger, not smaller.

The process of fault zone growth outlined here (Fig. 2) may provide a rationale for the rupture pattern observed on some seismogenic faults. The growth process involves the linkage of faults by the fracturing of progressively larger discontinuities: from centimeter-size at the small fault stage, to meter-size at the simple fault zone stage, to several meters at the compound stage. As adjacent segments become linked and a fault zone lengthens, displacement is transferred through the discontinuities. The spacing and size of the largest discontinuities becomes progressively greater. Wesnousky (1988) has noted that historic ruptures of several large strike-slip fault zones typically terminate at the widest steps along the trace of the rupture and that the spacing between the terminating steps increases as a function of the cumulative displacement across fault zones. These observations are consistent with the linkage process outlined above.

This process of fault zone growth outlined here may be common. Single systems of parallel fractures occur in a broad variety of rocks. Other kinds of planar anisotropies may also provide a mechanical fabric similar to the Mount Abbot joints. For example, the Fort Foster Brittle Zone (Swanson 1988), which developed in mylonitic host rocks, is in several ways similar to the compound fault zones described herein. Detailed mapping in other areas with strong planar penetrative fabrics is likely to show that many brittle fault zones form in a manner similar to the compound fault zones of the Bear Creek area.

CONCLUSIONS

The compound fault zones of the Bear Creek area grew from a pre-existing set of joints. These zones grew in length and displacement as faults of progressively larger length and spacing became linked by fractures. The sequence of fault zone development is not well described by typical 'Riedel shear' models. Discontinuities that at one point separated different fault zone segments are 'broken' and become internal features, presumably leaving discontinuities of equal or larger size at the 'new' fault zone ends. Although the Mount Abbot fault zones may become 'smoother' in the sense that the spacing of the largest discontinuities increases, they become rougher in the sense that the size of the discontinuities also increases. This model provides a mechanically consistent, field-based conceptual model for fault zones that grow in basement rocks. This growth process

may parallel the rupture pattern observed along some seismogenic faults.

Acknowledgements—This research was supported by National Science Foundation Grants EAR8417021 and EAR 8319431. This manuscript was completed at Lawrence Berkeley Laboratory, operated by the University of California for the Department of Energy under contract No. DE-AC03-76SF0098. I thank David Pollard for this thorough and insightful reviews during the evolution of this manuscript and Larry Mastin for his help with the fieldwork. The comments from Rick Sibson, Hal Wollenberg, Pat Williams and two anonymous reviewers for the *Journal of Structural Geology* also led to substantial improvements in the manuscript.

REFERENCES

Aydin, A. A. & Johnson, A. M. 1978. Development of faults as zones of deformation bands and as slip surfaces in sandstone. *Pure & Appl. Geophys.* **116**, 931–942.

Bartlett, W. L., Friedman, M. & Logan, J. M. 1981. Experimental folding and faulting of rocks under confining pressure—IX. Wrench faults in limestone layers. *Tectonophysics* **79**, 255–277.

Bilham, R. & King, G. 1989. The morphology of strike-slip faults; examples from the San Andreas fault, California. *J. geophys. Res.* **94**, 10,204–10,216.

Brace, W. F. & Bombolakis, E. G. 1963. A note on brittle crack growth in compression. *J. geophys. Res.* **68**, 3709–3713.

Chester, F. M. & Logan, J. M. 1986. Implications for the mechanical properties of brittle faults from observation of the Punchbowl fault zone, California. *Pure & Appl. Geophys.* **124**, 79–106.

Cloos, H. 1928. Experimenten zur Inneren Tektonik. *Zentbl. Miner. Geol. Palaeont. Abh. B*, 609–621.

Davis, G. H. 1984. *Structural Geology of Rocks and Regions*. Wiley, New York.

Davies, R. K. & Pollard, D. D. 1986. Relations between left-lateral strike-slip faults and right-lateral monoclinal kink bands in granodiorite, Mt. Abbot quadrangle, Sierra Nevada, California. *Pure & Appl. Geophys.* **124**, 177–201.

Engelder, J. T. 1974. Cataclasis and the generation of fault gouge. *Bull. geol. Soc. Am.* **85**, 1515–1522.

Engelder, J. T. 1987. Joints and shear fractures in rock. In: *Fracture Mechanics of Rock* (edited by Atkinson, B. K.). Academic Press, London, 27–69.

Erdogan, F. & Sih, G. C. 1963. On the crack extension in plates under plane loading and transverse shear. *J. Basic Engng* **85**, 519–527.

Hobbs, B. E. Means, W. D. & Williams. P. F. 1976. *An Outline of Structural Geology*. Wiley, New York.

Horii, H. & Nemat-Nasser, S. 1985. Compression-induced microcrack growth in brittle solids: axial splitting and shear failure. *J. geophys. Res.* **90**, 3105–3125.

Hundley-Goff, E. M. & Moody, J. B. 1980. Microscopic characteristics of orthoquartzite from sliding friction experiments. I. sliding surface. *Tectonophysics* **62**, 279–299.

Jackson, R. E. & Dunn, D. E. 1974. Experimental sliding friction and cataclasis of foliated rocks. *Int. J. Rock Mech. & Mining Sci.* **11**, 235–249.

Lockwood, J. P. & Lydon, P. A. 1975. Geologic map of the Mount Abbot quadrangle, California. *U.S. geol. Surv. Geol. Quadrangle* GQ–1155.

Logan, J. M., Friedman, M. Higgs, N. Dengo, C. & Shimamoto, T. 1979. Experimental studies of simulated gouge and their application to studies of natural fault zones. *U.S. geol Surv. Open-File Report* **79–1239**, 305–343.

Martel, S. J. & Pollard, D. D. 1989. Mechanics of slip and fracture along small faults and simple strike-slip fault zones in granitic rock. *J. geophys. Res.* **90**, 3105–3125.

Martel, S. J., Pollard, D. D. & Segall, P. 1988. Development of simple strike-slip fault zones, Mount Abbot quadrangle, Sierra Nevada, California. *Bull. geol. Soc. Am.* **100**, 1451–1465.

McKee, J. W., Jones, N. W. & Long, L. E. 1984. History of recurrent activity along a major fault in northeastern Mexico. *Geology* **12**, 103–107.

Meuhlberger, W. R. 1986. Different slip senses of major faults during different orogenies: the rule? In: *Proceedings of the 6th International Conference on Basement Tectonics*, International Basement Tectonics Association, 76–81.

Mitra, G. 1984. Brittle to ductile transition due to large strains along the White Rock thrust, Wind River Mountains, Wyoming. *J. Struct. Geol.* **6**, 51–61.

Naylor, M. A., Mandl, G. & Sijpesteijn. 1986. Fault geometries in basement-induced wrench faulting under different initial stress states. *J. Struct. Geol.* **8**, 737–752.

Noyes, H. J., Wones, D. R. & Frey, F. A. 1983. A tale of two plutons: petrographic and mineralogic constraints on the petrogenesis of the Red Lake and Eagle Peak plutons, central Sierra Nevada, California. *J. Geol.* **91**, 353–379.

Pollard, D. D. & Segall, P. 1987. Theoretical displacements and stresses near fractures in rocks: with applications to faults, joints, veins, dikes, and solution surfaces. In: *Fracture Mechanics of Rock* (edited by Atkinson, B. K.). Academic Press, London, 277–349.

Price, N. J. 1981. *Fault and Joint Development in Brittle and Semi-brittle Rock*. Pergamon Press, Oxford.

Ramsay, J. G. 1980. Shear zone geometry: a review. *J. Struct. Geol.* **2**, 83–99.

Riedel, W. 1929. Zur Mechanik geologischer Brucherscheinungen. *Zentbl. Miner. Geol. Palaeont. Abh. B.* 354–368.

Robertson, E. C. 1983. Relationship of fault displacement to gouge and breccia thickness. *Mining Engng* **35**, 1426–1432.

Scholz, C. H. 1987. Wear and gouge formation in brittle faulting. *Geology* **15**, 493–495.

Segall, P. & Pollard, D. D. 1980. Mechanics of discontinuous faults. *J. geophys. Res.* **85**, 4337–4350.

Segall, P. & Pollard, D. D. 1983a. Joint formation in granitic rock of the Sierra Nevada. *Bull. geol. Soc. Am.* **94**, 563–575.

Segall. P. & Pollard, D. D. 1983b. Nucleation and growth of strike-slip faults in granite. *J. geophys. Res.* **88**, 555–568.

Segall, P. & Simpson, C. 1986. Nucleation of ductile shear zones on dilatant fractures. *Geology* **14**, 56–59.

Sibson, R. H. 1977. Fault rocks and fault mechanisms. *J. geol. Soc. Lond.* **133**, 191–213.

Sibson, R. H. 1986. Earthquakes and rock deformation in crustal fault zones. *Annu. Rev. Earth & Planet. Sci.* **14**, 149–175.

Sibson, R. H., White, S. H. & Atkinson, B. K. 1981. Structure and distribution of fault rocks in the Alpine fault zone, New Zealand. In: *Thrust and Nappe Tectonics* (edited by McClay, K. & Price, N. J.). *Spec. Publs geol. Soc. Lond.* **9**, 197–210.

Stern, T. W., Bateman, P. C., Morgan, B. A., Newell, M. F. & Peck, D. L. 1981. Isotopic U–Pb ages of zircon from the granitoids of the central Sierra Nevada, California. *Prof. Pap. U.S. geol. Surv.* **1185.**

Suppe, J. 1985. *Principles of Structural Geology*. Prentice-Hall. Englewood Cliffs, New Jersey.

Swanson, M. T. 1988. Pseudotachylyte-bearing strike-slip duplex structures in the Fort Foster Brittle Zone of southernmost Maine. *J. Struct. Geol.* **10**, 813–828.

Sylvester, A. G. 1988. Strike-slip faults. *Bull. geol. Soc. Am.* **100**, 1666–1703.

Tchalenko, J. S. 1968. The evolution of kink-bands and the development of compression textures in sheared clays. *Tectonophysics* **79**, 255–277.

Tchalenko, J. S. 1970. Similarities between shear zones of different magnitudes. *Bull. geol. Soc. Am.* **81**, 1625–1640.

Tchalenko, J. S. & Ambraseys, N. N. 1970. Structural analysis of the Dasht-e-Bayaz (Iran) earthquake fractures. *Bull. geol. Soc. Am.* **81**, 41–60.

Wallace, R. E., & Morris, H. T. 1986. Characteristics of faults and shear zones in deep mines. *Pure & Appl. geophys.* **124**, 107–125.

Wesnousky, S. G. 1988. Seismological and structural evolution of strike-slip faults. *Nature* **335**, 340–343.

Wilcox. R. E., Harding, T. P. & Seeley, D. R. 1973. Basic wrench tectonics. *Bull. Am. Soc. Petrol. Geol.* **57**, 74–96.